RESEARCH

RESEARCH: Short Communication

Stretchable and fatigue-resistant materials

Chunping Xiang [1,2], **Zhengjin Wang** [1,2], **Canhui Yang** [2,3], **Xi Yao** [2,4], **Yecheng Wang** [2], **Zhigang Suo** [2,*]

[1] State Key Laboratory for Strength and Vibration of Mechanical Structures, School of Aerospace Engineering, Xi'an Jiaotong University, Xi'an 710049, China
[2] John A. Paulson School of Engineering and Applied Sciences, Kavli Institute for Bionano Science and Technology, Harvard University, Cambridge, MA 02138, USA
[3] Department of Mechanics and Aerospace Engineering, Southern University of Science and Technology, Shenzhen, Guangdong 518055, China
[4] Key Lab for Special Functional Materials of Ministry of Education, Henan University, Kaifeng, Henan 475004, China

In developing a material for a load-bearing application, attention inevitably falls on the resistance of the material to the growth of a crack, characterized by toughness under monotonic load, and by threshold under cyclic load. Many methods have been discovered to enhance toughness, but they do not enhance threshold. For example, stretch-induced crystallization and inorganic fillers have made the toughness of natural rubber well above $10000 \, J/m^2$, but have left the threshold of natural rubber around $50 \, J/m^2$. Here we describe a principle of stretchable and fatigue-resistant materials. To illustrate the principle, we embed unidirectional fibers of a soft and stretchable material in a matrix of a much softer and much more stretchable material, and adhere the fibers and the matrix by sparse and covalent interlinks. When the composite is cut with a crack and subject to a load, the soft matrix shears readily and delocalizes the high stretch of a fiber over a long segment. A threshold of $1290 \, J/m^2$ is reached, below which the composite does not suffer any mode of failure (fiber break, kink crack, or matrix fracture). The principle of stretchable and fatigue-resistant materials is applicable to various materials, layouts, and methods of fabrication, opening an enormous design space for general applications.

Introduction

Stretchable materials—elastomers, hydrogels, organogels, and ionogels, along with their hybrids—are fundamental to numerous and far-reaching applications. Examples include tissue repair [1], drug delivery [2], soft robots [3,4], ionotronics [5–7], bioelectronics [8–10], synthetic biology [11], skin-attached and implanted devices [12], as well as wearable and washable active textiles [13,14]. In a load-bearing application, a material must resist the growth of a crack, characterized by toughness Γ under monotonic load, and threshold Γ_{th} under cyclic load [15]. We plot representative data on the toughness–threshold chart

(Fig. 1). The diagonal of the chart represents materials having equal toughness and threshold. This ideal behavior approximately describes materials that do not have potent tougheners, such as ceramics: they are brittle but fatigue-resistant. Most load-carrying materials—plastics, metals, elastomers, hydrogels—have potent natural or engineered tougheners, and fall much below the diagonal: these materials are tough but fatigue-prone. For these tough materials, the threshold is typically lower than the toughness by one to two orders of magnitude. A salient example is natural rubber, which has toughness above $10000 \, J/m^2$, but threshold around $50 \, J/m^2$ [16].

A stretchable material undergoes large and reversible deformation by the entropic elasticity of a covalent polymer network. A conflict exists in developing such a stretchable material: the

* Corresponding author.
 E-mail address: Suo, Z. (suo@seas.harvard.edu)
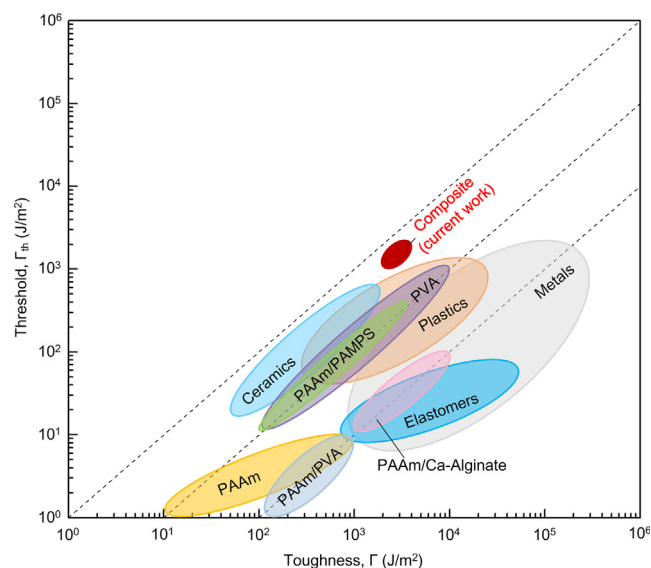
FIGURE 1

The threshold-toughness chart approximately locates various classes of materials. The chart is constructed using recently obtained data of hydrogels: PAAm [17,18], PAAm/PVA [19], PAAm/Ca-Alginate [20], PAAm/PAMPS [21], and PVA [22,23], along with data of established load-bearing materials (elastomers, plastics, metals, and ceramics) [24]. The composite of this work achieves a threshold about 1300 J/m^2 and a toughness about 4000 J/m^2.

covalent polymer network cannot achieve both high crack resistance and high elastic modulus. As the number of monomer units per chain, n, increases, the toughness and threshold increase $\Gamma \sim \Gamma_{th} \sim n^{1/2}$, but the elastic modulus decreases, $\mu \sim n^{-1}$ [16]. Consequently, pure single-network materials rarely fit for load-bearing applications. Methods have been developed to enhance toughness under monotonic load by introducing sacrificial bonds (i.e., tougheners), such as covalent networks of short polymer chains [25,26], noncovalent complexes [27], and inorganic fillers [28,29]. These tougheners, however, do not change the scaling for the threshold, $\Gamma_{th} \sim n^{1/2}$ [16,20,21,30]. A recent study has uncovered that double-network hydrogels achieve threshold of hundreds of J/m^2 [21]. The short-chain network greatly improves strength and stiffness, allowing the long-chain network to have an extraordinarily large value of n, and thereby increasing the threshold. In separate recent studies, poly-vinyl alcohol hydrogels form crystalline domains, exhibit flaw insensitivity [31], and achieve threshold about 1000 J/m^2 [22,23]. This approach, however, is limited to special materials.

We have recently described a principle of stretchable and tough materials without using sacrificial bonds [32]. In that work we reconciled the conflict between toughness and hysteresis, achieving both high toughness and low hysteresis. The principle requires that the fibers should be stiffer than the matrix; and the interface adhesion between fibers and the matrix should be strong. This work focuses on the fatigue resistance of materials. We demonstrate that the above principle is also critical for enhancing fatigue resistance of materials. Beyond that, high resistance to shear deformation of matrix and large feature size are necessary as well. To illustrate the principle, we embed unidirectional fibers of a soft and stretchable material in a matrix of

much softer and much more stretchable material, and adhere the fibers and the matrix by sparse and covalent interlinks (Fig. 2). Both materials are elastic, with low hysteresis. When the composite is cut with a crack by a razor blade and subject to a cyclic load, the soft matrix shears greatly and delocalizes the high stretch of a fiber over a long segment. Consequently, the composite requires more energy to grow the crack than a homogeneous material. In the limit when the matrix vanishes, all fibers share the load, and the rest of the composite is completely unaffected by the razor-cut crack. In practice, of course, a matrix is needed to bind the fibers into a solid material.

The principle breaks the conflict between crack resistance and elastic modulus. The fibers and matrix have different polymer chain lengths, and can be made of dissimilar polymers. The matrix has a polymer network of long chains, and therefore has low modulus and high threshold. The matrix does not carry much load, and sustains large shear deformation at the tip of the precut crack, without growing a kink crack. Each fiber has a polymer network of short chains, and therefore has high modulus and low threshold. Because the soft matrix deconcentrates stress in the fiber, the threshold of the composite can be much higher
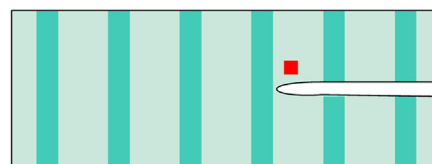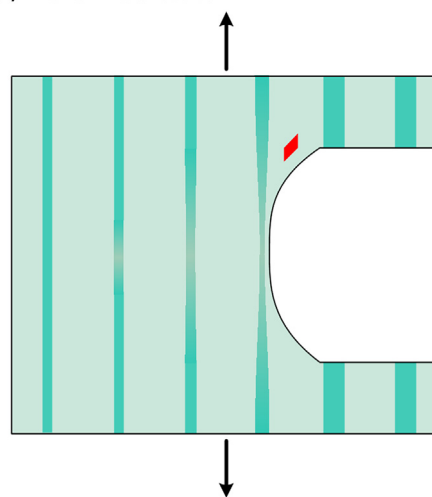
FIGURE 2

Principle of stretchable and fatigue-resistant materials. (a) Undeformed state. Unidirectional fibers of a soft and stretchable material are embedded in a matrix of much softer and much more stretchable material. The fibers adhere to the matrix through sparse and covalent interlinks. The composite is cut with a crack using a razor blade. A small piece of the matrix is marked by a red square. (b) Deformed state. When an applied force stretches the composite, the matrix shears greatly, deforms the red square into a parallelogram, blunts the crack, and delocalizes the high stretch of a fiber over a long segment. Strong fiber–matrix adhesion prevents sliding and separation.

FIGURE 3

Snapshots of a crack in a composite subject to cyclic load of stretch of amplitude 1.725 and energy release rate of amplitude 1290 J/m^2. The undeformed composite has a crack cut by a razor blade. The long edges of the composite are clamped by rigid gripers. When the loading machine moves the gripers cyclically, the crack extends slightly to the first fiber ahead in several thousand cycles, and then stops without further extension over 30000 cycles. The shape of the crack remains nearly unchanged between the last two snapshots.

than that of the fiber. The sparse and covalent fiber–matrix interlinks prevent debonding and sliding, and yet allow the composite to be stretchable.

Composites of materials of high modulus contrast and strong interface adhesion have long been developed. Examples include glass or carbon fibers in epoxy matrices [33], strong threads in elastomers [34], brick–mortar materials [35], strong fibers and mats in hydrogels [36,37], and heterogeneous adhesives [38]. These materials, however, are not stretchable. Composites have been made of patterned hard material in a soft matrix [39,40]. Such a material can also be stretchable and fatigue-resistant. Here we focus on composites made of all stretchable materials.

Results and discussion

The principle of stretchable and fatigue-resistant materials is general, applicable to various materials, layouts, and methods of fabrication, so long as the constituents fulfill the basic requirements outlined above. We demonstrate the principle by embedding fibers of a polydimethylsiloxane (PDMS) elastomer into a matrix of a polyacrylamide (PAAm) hydrogel. We choose these materials mainly because they fulfill the basic requirements and are easy to

fabricate in our laboratory, letting us test ideas with convenience. See Experimental section for details about fabrication. The shear modulus of the elastomer (401.35 kPa) is about two orders of magnitude higher than the shear modulus of the hydrogel (2.73 kPa). The elastomer ruptures at a stretch about 2, and the hydrogel ruptures at a stretch about 10. We adhere the fibers and the matrix by sparse covalent interlinks, so that the adhesion is strong, but does not lower stretchability of the fibers. The elastomer is hydrophobic, and does not absorb water from the hydrogel, so that the two materials in contact are stable. The fibers have the width of 2.5 mm and the spacing of 3.75 mm. The thicknesses of the fibers and the composites are 0.5 mm and 1.1 mm, respectively, giving a fiber-content of 20.3% by weight.

We prepare a long rectangular composite, clamp the long edges using long grippers, cut the composite with a crack using a razor blade, and subject the composite to cyclic stretch of a prescribed amplitude λ_m (Fig. 3). See Experimental section for detail. Because the composite has near perfect elasticity except for a region around the crack tip, the amplitude of stretch gives the amplitude of energy release rate, G. The composite with a precut crack survives over 30000 cycles of load with the amplitude of energy release rate of 1290 J/m^2. By comparison, the toughness is 365 J/m^2 for the elastomer, 1142 J/m^2 for the hydrogel, and 4136 J/m^2 for the composite. The precut crack propagates slightly before meeting the first fiber in front in several thousand cycles, then stops and keeps a stable shape in the rest of cycles.

We also stretch the elastomer, hydrogel, and composite with no precut crack over 20000 cycles. The stress–stretch loops and the dissipated energy per unit volume in each cycle of the three materials change somewhat in initial cycles, but are stable subsequently (Fig. 4).

Subject to a cyclic load of sufficiently high amplitude, the composite develops several modes of failure, including fiber break, kink crack, and matrix fracture (Fig. 5). For a composite with a matrix much softer and much more stretchable than the fibers, fiber break occurs prior to the other modes of failure. We subject samples of a composite to cyclic loads of various prescribed amplitudes of energy release rate, and record the number of cycles when each sample breaks a fiber. A fiber breaks in the first cycle when a sample is under the energy release rate of 4441 J/m^2 (Fig. 6a). The composite survives more cycles under smaller amplitudes of energy release rate (Fig. 6b and c). If the amplitude of energy release rate is further decreased, the composite can survive after tens of thousands of cycles without fiber break (Fig. 6d and e).

We plot the amplitude of energy release rate against the number of cycles at the observation of a failure mode (Fig. 6f). By a failure mode we mean a visible damage such as fiber break, kink crack, and matrix fracture. Such a G–N curve characterizes the behavior of a composite containing a precut crack in response to cyclic loads. We define the toughness by the energy release rate that causes a failure mode in the first cycle (N = 1). We define the threshold by the amplitude of energy release rate below which the composite remains stable for infinite number of cycles. Ideally, many samples should be cycled at each amplitude of energy release rate to ascertain failure statistics, and should be tested over infinite number of cycles at small amplitude of energy
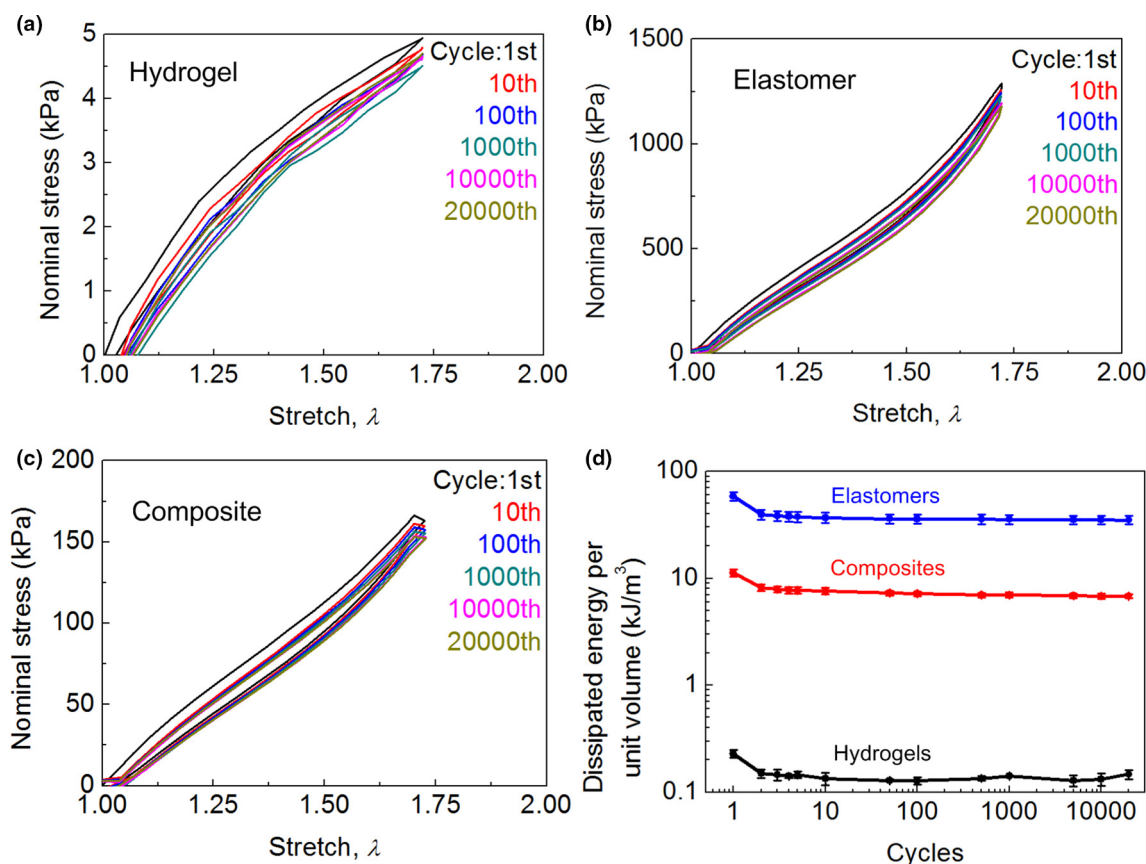
FIGURE 4

Cyclic stress–stretch curves for samples with no precut cracks: (a) hydrogel, (b) elastomer, and (c) composite. (d) Dissipated energy per unit volume as a function of the number of cycles. Each data point represents the mean of 3 experimental results. The error bars represent standard deviation.

release rate to locate the threshold. In practice, one can stretch a material only by a finite number of cycles. If the G–N curve approaches an asymptote as the number of cycles increases, the asymptote defines the threshold. The concept is analogous to the endurance limit of the stress-cycle (S–N) curve. Characterizing the fatigue behavior of a material takes a long time, and some compromise is inevitable. To illustrate the method of G–N curve, here we test a total of sixteen samples. No damage is observed when the composite is stretched for 30000 cycles with amplitude of energy release rate of 1290 J/m^2. We take this value as an estimate of the threshold of the composite. Note that the slight propagation of crack before meeting the first fiber in front is allowed in defining the fatigue threshold of the composite, as it will be stopped by the fiber and barely affects the load-bearing capacity and integrity of the composite. Also note that no crack propagation is allowed in defining the fatigue threshold of homogeneous materials. Nevertheless, such difference is negligible so far as the load-carrying capacity is concerned, and it is reasonable to compare the fatigue threshold of the composite and other homogeneous materials in Fig. 1.

The thresholds of hydrogels and elastomers have been extensively studied. The threshold of hydrogel is between 4.19 J/m^2 [17] and 418 J/m^2 [21], depending on the water content and crosslink density. The threshold of hydrogel used in this work is within this range. The threshold of most elastomers is in the range of 50–100 J/m^2 [24]. The measured threshold of the

composite is 1290 J/m^2, which is one order higher than the threshold of its constituent materials. As noted in the Introduction of the paper, an elastic modulus–threshold conflict exists in single-network elastomers and single-network hydrogels. The hydrogels of high threshold have small elastic modulus, and cannot carry much load. The composites resolve this elastic modulus–threshold conflict, and have both high elastic modulus and high threshold.

The composite fails by forming a kink crack when the matrix is not so stretchable. We make a composite with a matrix of a PAAm hydrogel of much less stretchability (1.56 of the sample with a precut crack), and then observe the composite under the cyclic load of the amplitude of energy release rate of 1290 J/m^2 (Fig. 7). The precut crack propagates obviously in the first cycle until meets the first fiber ahead. A kink crack initiates in 6414 cycles. The kink crack grows in the rest of cycles and the matrix also fails near a gripper. Meanwhile, another kink crack initiates and propagates in the rest of cycles.

For composite with highly stretchable matrix, kink crack also forms as the feature size of the composite reduces (Fig. 8). We increase the number of fibers and decrease the width of fibers, but keep the fiber-content unchanged (20.3 wt%). Under the same amplitude of energy release rate of 1290 J/m^2, the precut crack propagates slowly until it meets the first fiber ahead in 6432 cycles. A kink crack initiates in 10317 cycles and propagates upward in the rest of cycles. The smaller feature size leads to

**(a) Fiber break**   **(b) Kink crack**   **(c) Matrix fracture**
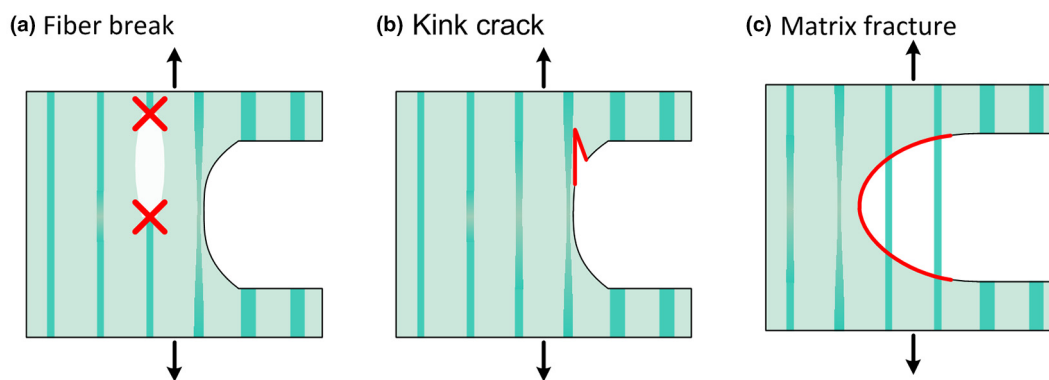
FIGURE 5

Schematics of three modes of failure observed in the composites.

larger shear deformation of the matrix near the crack tip even under the same applied energy release rate.

A composite fails by a matrix fracture when the matrix-fiber adhesion is weak. We prepare two groups of composites. In one group, the elastomer and the hydrogel form covalent interlinks. In the other group, the elastomer and the hydrogel contact by noncovalent interaction. The two groups show different stress–stretch curves (Fig. 9a and b). The toughness of the composites with strong interface adhesion is about fourfold of that with weak interface adhesion (Fig. 9c).

The precut crack can propagate easily at a relatively small stretch (about 1.59) in a neat hydrogel of less stretchability (Video 1). Similarly, for a composite with weak fiber–matrix adhesion, the precut crack keeps propagating, while the fibers remain intact, leading to a critical stretch (about 1.65) similar to that of the neat hydrogel (Video 2). On the contrary, for the composite with strong matrix-fiber adhesion, the growth of the precut crack is prohibited by the fibers, leading to obvious increase of the critical stretch (about 2.05. Video 3).
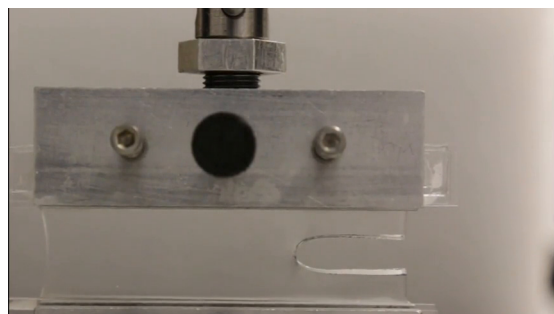
Video 1.
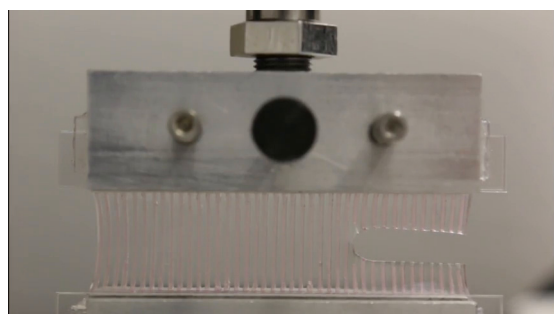
Video 2.
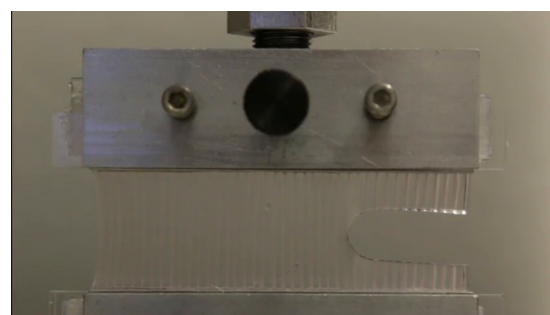
Video 3.

We have demonstrated a principle of stretchable and fatigue-resistant materials through elastomer–hydrogel composite. Here we show some theoretical understandings to discuss the essential mechanics responsible for the enhancement of threshold. For an extreme case of the composite when the matrix vanishes, like a rope with many threads, all the fibers (threads) share the applied load, the existence of a crack has no effect on the remaining fibers. There is no stress concentration in the fibers, and the fatigue threshold of the composite is limited by the endurance limit of fiber material and fiber length, i.e., $\Gamma_{th} = W_e L$, where W_e is the endurance energy density of the constituent material of fibers, L is the length of fibers. This should be applicable to all materials. For metals, the endurance stress limit is at the order of 100 MPa [41,42] and their modulus is at the order of 100 GPa, giving the endurance energy density at the order of 10^5 J/m^3, a fiber length of 1 cm leads to a fatigue threshold of 1000 J/m^2. Much longer fibers will increase the fatigue threshold dramatically. In engineering, steel wire ropes can bear the weight of a bridge under fluctuating loads over many years. For materials of small feature size, like micro-truss materials [43], it is well known the endurance limit of material increases as the fiber diameter decreases. The material may also have large fatigue threshold.

In most cases, a matrix is needed to bind the fibers into a solid material. As long as the matrix is much softer than the fibers, a crack in matrix will not cause severe stress concentration in the fibers and affects their endurance. Unconfined matrix damage, like kink crack and matrix fracture, will limit the threshold of composites. Strong interface adhesion between the fibers and matrix prevents the matrix fracture. Kink crack is limited by the endurance to large shear deformation of matrix. Unconfined

matrix damage may be governed by the toughness of matrix [31] or flaw sensitivity of matrix [44], which is unclear at present and remains to be explored.
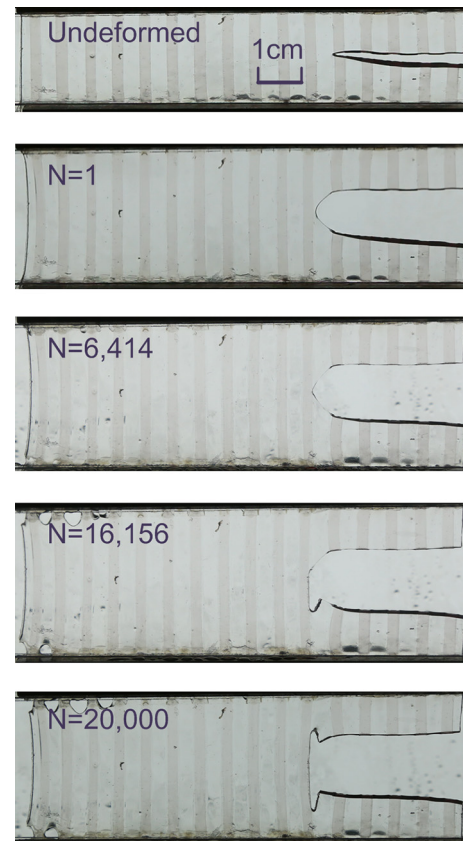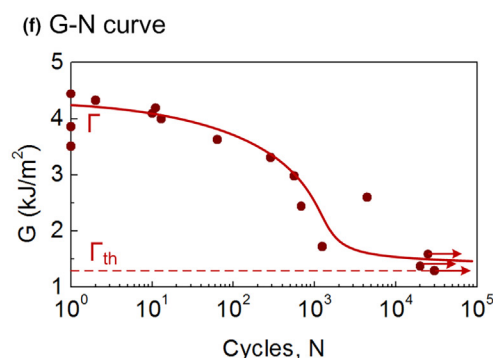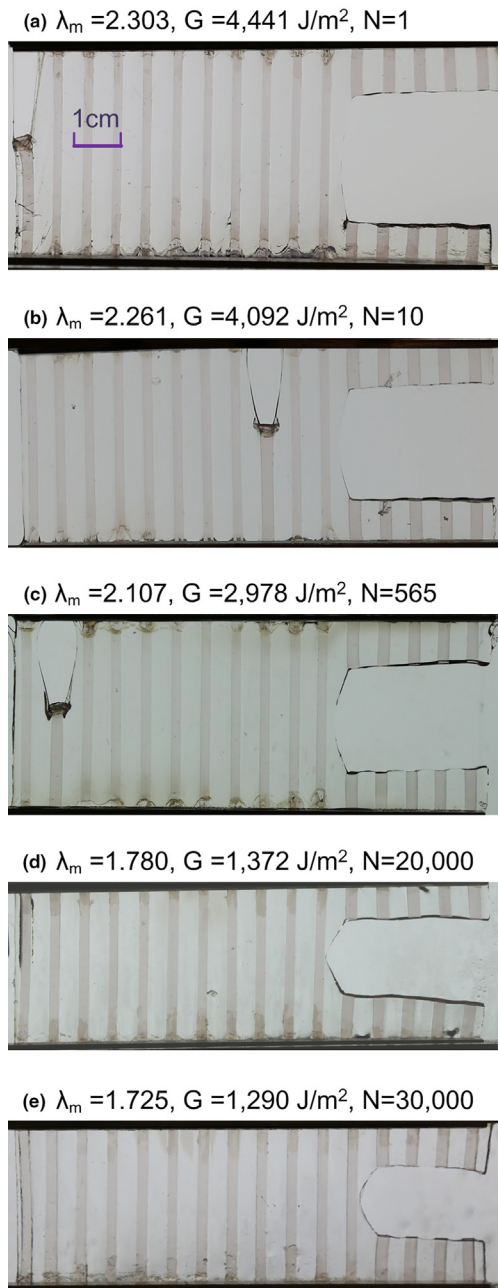

(a) λ_m =2.303, G =4,441 J/m², N=1

(b) λ_m =2.261, G =4,092 J/m², N=10

(c) λ_m =2.107, G =2,978 J/m², N=565

(d) λ_m =1.780, G =1,372 J/m², N=20,000

(e) λ_m =1.725, G =1,290 J/m², N=30,000

(f) G-N curve

FIGURE 7

Fatigue behavior of a composite when the matrix is not so stretchable. The composite forms a kink crack and matrix rupture at the boundary after about 6000 cycles under an amplitude of energy release rate of 1290 J/m².

Concluding remarks

Stretchable and fatigue-resistant materials are important for many applications. Most existing toughening methods enhance toughness under monotonic loads, but not the threshold under cyclic loads. We demonstrate a principle of stretchable and fatigue-resistant materials. The principle requires that (i) the matrix should be much softer than the fibers, (ii) the interface adhesion between the fibers and matrix should be strong, (iii) the matrix should be resistant to large shear deformation, and (iv) the feature size should be large enough. These requirements enhance threshold, below which a composite survives cyclic
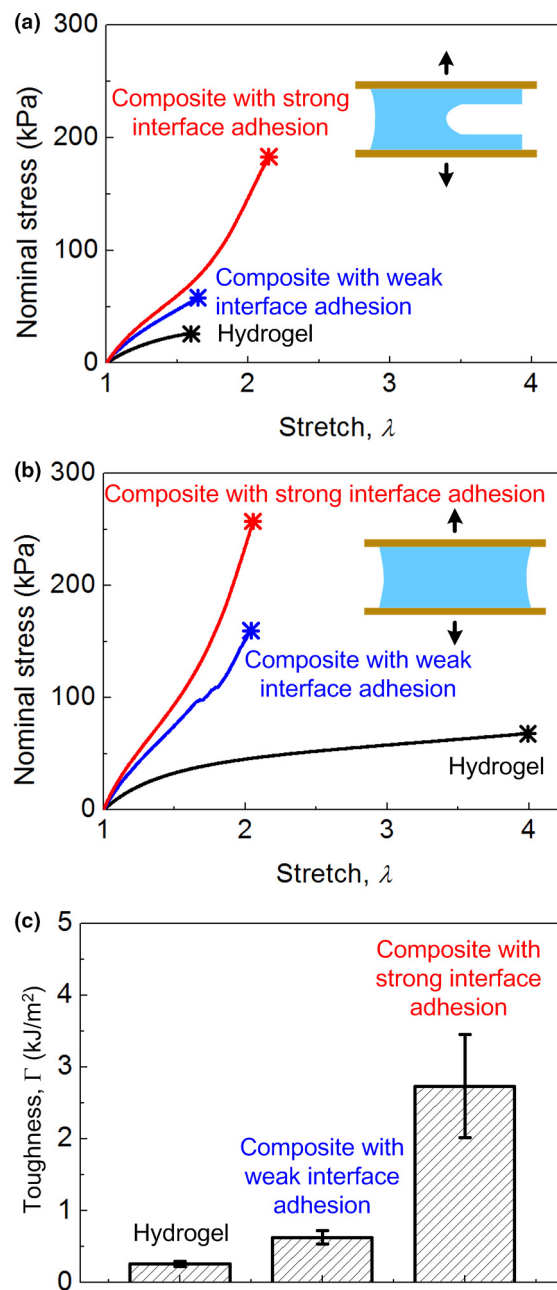
FIGURE 6

The number of cycles to fail a composite tested at various amplitudes of energy release rate. Each sample is cut with a crack using a razor blade. (a) A sample fails by fiber break in the first cycle at an energy release rate of 4441 J/m². (b and c) As the amplitude of energy release rate reduces, the number of cycles at the observation of failure increases. (d and e) When the amplitude of energy release rate is sufficiently low, no damage is observed when the experiments are terminated. (f) The G–N curve of the composite. Each dot records the number of cycles at a prescribed amplitude of energy release rate. Each arrow records a sample that survives a certain number of cycles of stretch at a prescribed amplitude of energy release rate, without any modes of failure. The solid line is a guide to the eye.

RESEARCH: Short Communication
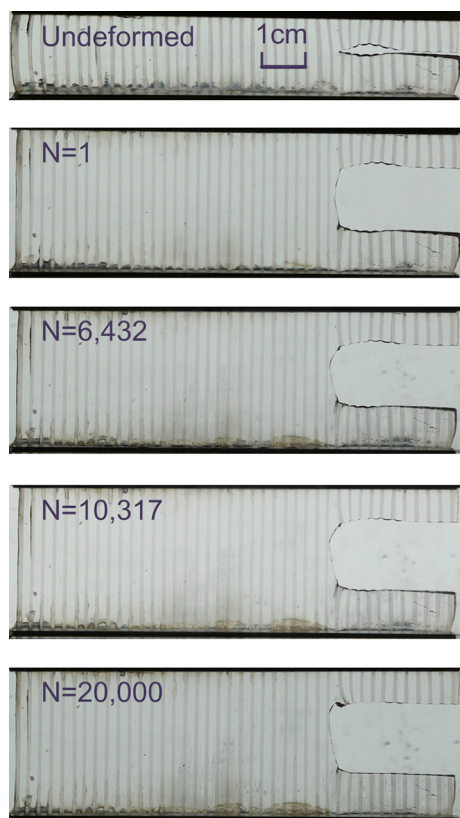
FIGURE 8

Fatigue behavior of a composite with small feature size. A kink crack forms after about 10000 cycles under an amplitude of energy release rate of 1290 J/m^2.

loads without suffering any mode of failure (fiber break, kink crack, or matrix fracture).

We have demonstrated the principle using a specific pair of stretchable materials (an elastomer and a hydrogel), a specific layout (unidirectional fibers in a matrix), and a specific method of fabrication (See Experimental section). But the principle is general. Other stretchable materials, layouts, and methods of fabrication can also achieve high fatigue threshold, with additional attributes desired in applications. Elastomer–hydrogel composites can store and transport small molecules and ions, and can be used for drug delivery and ionotronics. Hydrogel-hydrogel composites can have large water content and large range of stiffness. Hydrogel-tissue composites can be used in tissue regeneration. The principle of fatigue-resistant materials does not require specific layouts of the two constituents of large stiffness contrast. A composite of unidirectional fibers is anisotropic and resists crack in one direction. A laminate of multidirectional fibers is approximately isotropic in plane and resists cracks in many in-plane directions. A composite of three-dimensional fiber networks can be isotropic in macro-scale and resists crack in all directions. Methods of fabrication include fiber spin [45], extrusion print [46], and stereolithography [47]. Both hydrogel and elastomer are compatible with these methods. One can choose the most suitable fabrication on demand. The art of adhesion has undergone transformative advances in recent years, enabling—in principle—tough and stretchable adhesion

FIGURE 9

Effects of fiber–matrix adhesion. Nominal stress–stretch curves for hydrogel and composites with weak and strong interface adhesion of (a) notched samples and (b) unnotched samples. The stars represent the rupture. The thicknesses of fibers and the composites are 0.5 mm and 3.05 mm, respectively. The fibers have the width of 1 mm and the spacing of 2.5 mm, giving a fiber-content of 7.35 wt%. Hydrogels have same size as the composites. (c) Toughness of the hydrogels and the composites with weak and strong interface adhesion. The data represents the mean of 3 experimental results. The error bars represent standard deviation.

between any pair of stretchable materials [48]. The diversity in materials, layouts, and methods of fabrication provide an enormous design space to develop stretchable and fatigue-resistant materials. It is hoped that this class of materials will enable new technologies where pre-longed cyclic loads prevail, such as cartilage replacements and artificial heart valves in healthcare and soft robots and wearable devices in engineering.
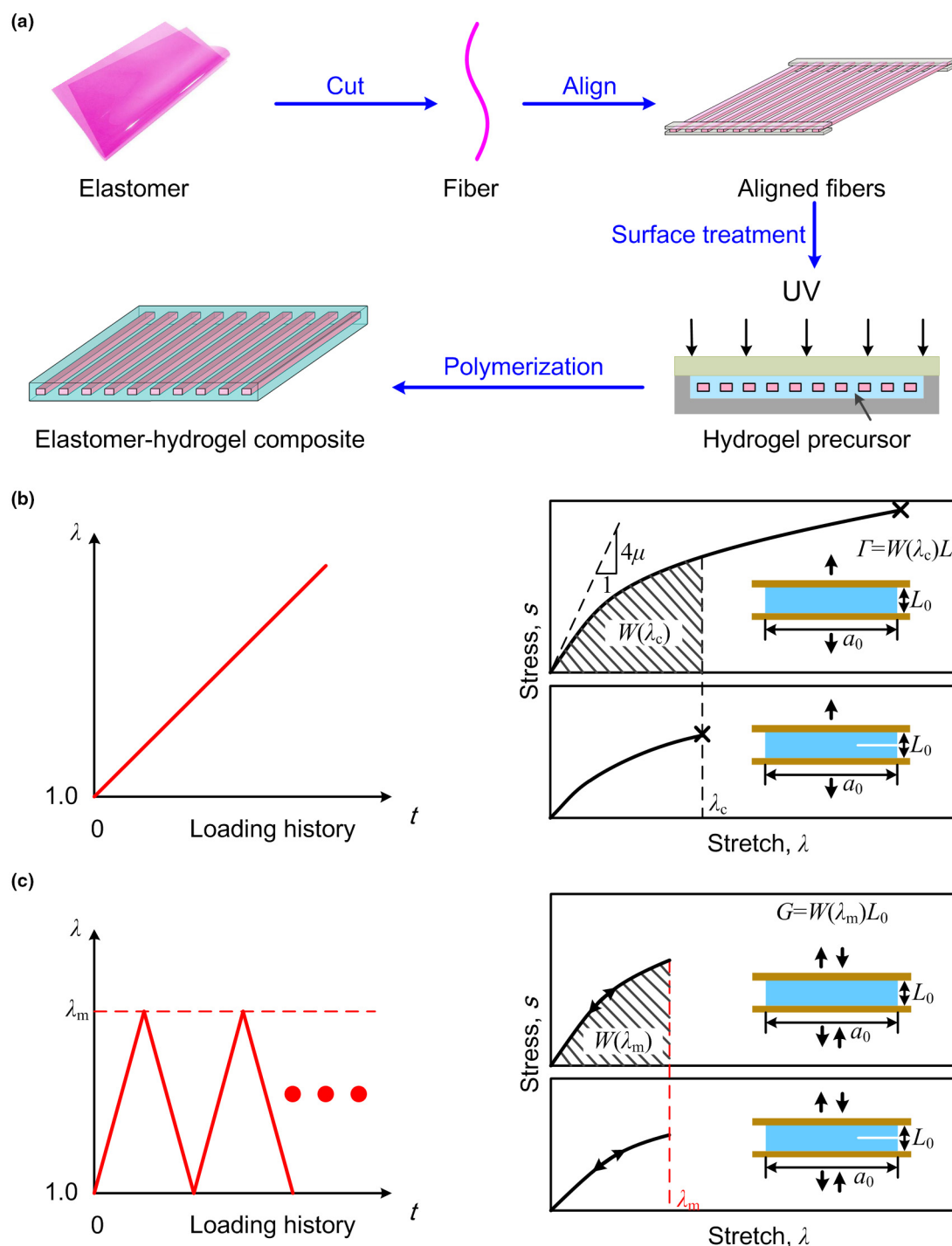
RESEARCH: Short Communication

FIGURE 10

Fabrication of elastomer–hydrogel composites and measurement of mechanical properties.

Experimental section

Synthesis of PAAm hydrogels

Acrylamide (AAm; Sigma-Aldrich, A8887) was dissolved in distilled water (Poland Spring) to form an aqueous solution of the monomer. Two concentrations were selected, with 30% and 12.45% AAm by weight. N,N′-Methylenebisacrylamide (MBAA; Sigma-Aldrich, M7279) was dissolved in distilled water to form a solution with nominal concentration of 0.1 M MBAA as cross-

linker. 2-Hydroxy-4′-(2-hydroxyethoxy)-2-methylpropiophenone (I2959; Sigma-Aldrich, 410896) was dissolved in ethyl alcohol (Sigma-Aldrich, 459844) to form a solution with nominal concentration of 0.1 M I2959 as photoinitiator. The hydrogel precursor was made by mixing the monomer, crosslinker, and photoinitiator. To make a less stretchable hydrogel, we added 9.6 µL crosslinker and 4.8 µL photoinitiator into every 1 g of the AAm solution (30 wt%). To make a highly stretchable

hydrogel, we added 4 μL crosslinker and 1.5 μL photoinitiator into every 1 g of the AAm solution (12.45 wt%). Then the precursor was poured into a mold made of laser-cut acrylic and covered by a glass sheet with thickness of 6.25 mm (McMaster-Carr). Thereafter, the mold was placed under an ultraviolet lamp (15 W 365 nm; UVP XX-15L, 7 cm distance between sample and lamp) for 1 h for polymerization. We kept the hydrogels in the sealed mold for 12 h at room temperature for exhausting monomers and initiator before tests.

Synthesis of PDMS
The precursor of PDMS was made by mixing the base and the curing agent of Sylgard 184 (Dow Corning) at 10:1 weight ratio with 1% v/w of red airbrush color (Createx). The mixed precursor was poured into a mold made of acrylic. The precursor was then degassed by a vacuum pump for 30 min for the air bubbles to float out. Subsequently, the mold and the precursor were covered with an acrylic sheet and placed at 65 °C in an oven (VWR, Model No. 1330GM) for 12 h. The thickness of as-prepared PDMS membrane is 0.5 mm.

Preparation of PDMS fibers
The as-prepared PDMS membrane was fixed on a graph paper and cut by a paper cutter (Fig. 10a). The nominal width of the fibers is 1 mm for composites of small feature size or 2.5 mm for composites of large feature size. For making composites, the prepared PDMS fibers were aligned uniformly, and each end of them were bonded between two polycarbonate sheets by silicone sealants (3 M) to form a fiber-scaffold. The fiber-scaffold was kept at room temperature for 24 h to cure the silicone sealants.

Synthesis of elastomer–hydrogel composites
We realized tough and stretchable fiber–matrix adhesion by forming sparse and covalent interlinks using a photoinitiator (benzophenone) [49]. The fiber scaffolds were cleaned with ethyl alcohol and dried with pressured air. Then, the scaffold was immersed into benzophenone (Sigma-Aldrich, B9300) solution (10 wt% in Ethyl alcohol) for 2 min at room temperature. Thereafter, the scaffold was washed with ethyl alcohol and dried with pressured air. To make composites with weak interface adhesion, the scaffolds were just cleaned with ethyl alcohol and dried with pressured air without benzophenone treatment. The scaffold was fixed into a mold made of acrylic. The hydrogel precursor was poured into the mold. The fibers were soaked by the precursor. Then, the mold and the precursor were covered with a glass sheet and placed under the ultraviolet lamp for 1 h for polymerization (Fig. 10a). We kept the composites in the sealed mold for 12 h at room temperature.

Mechanical tests
Each sample of the hydrogel, elastomer, and composite was glued between two gripers (Fig. 10). In the undeformed state, the sample had width of $a_0 = 100$ mm, and length between two gripers of $L_0 = 20$ mm. The thicknesses of elastomers, hydrogels, and composites were 0.5 mm, 1.5 mm, and 1.1 mm, respectively, unless otherwise specified. During the tests, the samples were loaded by a mechanical testing machine (Instron model 5966) with a load cell of 100 N or 10 kN. The experimental process was recorded by a digital camera (Canon EOS 70D).

We used monotonic load for measuring the critical stretch, shear modulus, and toughness of stretchable materials (Fig. 10b). Three groups of samples were prepared to get the mean value and scatter of the measured mechanical properties. Each group had two identical samples. The notched sample with a 30 mm precut crack was used to measure the critical stretch, λ_c, while the unnotched sample was used to measure the stress–stretch curve. The nominal stress, s, is defined as the applied force divided by the cross-sectional area in the undeformed state. The stretch, λ, is defined as the current length between two grippers divided by the initial length. The stretch rate was 0.02 s^{-1}. The shear modulus, μ, is determined by the initial slop of the stress–stretch curve, and the toughness is calculated as $\Gamma = W(\lambda_c)L_0$, where $W(\lambda_c) = \int_1^{\lambda_c} s d\lambda$. It is noted that the failure mode of elastomer–hydrogel composites with strong interface adhesion is fiber break regardless of whether there is a precut crack. In principle, the critical stretch measured by the notched samples, λ_{cn}, is the same as that measured by the unnotched samples, λ_{cu}, which is also same as the stretchability of fibers. We choose the minimum of λ_{cn} and λ_{cu} as the measured critical stretch in the present experiments.

We use cyclic loading for measuring the fatigue behaviors of stretchable materials (Fig. 10c). During the test, the minimum stretch per unit cycle is controlled as 1. The amplitude of stretch, λ_m, depends on the applied energy release rate. The energy release rate was calculated from the stress–stretch curves of unnotched samples of first cycle, as $G = W(\lambda_m)L_0$, where $W(\lambda_m) = \int_1^{\lambda_m} s d\lambda$. The loading–unloading frequency is controlled roughly as 0.5 Hz. We recorded the force–displacement curves of the unnotched samples over cycles to evaluate their fatigue damage. While we measured the crack growth or failures of the notched samples over cycles to evaluate their fatigue fracture. During the tests, we used an acrylic chamber to minimize dehydration of hydrogels and elastomer–hydrogel composites. We controlled the relative humidity between 88% and 90% through a humidifier and a humidity controller (Zoo Med). All the samples of hydrogels and composites were weighed before and after the tests, and the weight change did not exceed 5%. The mechanical properties of the elastomer–hydrogel composites are represented by the properties on the direction parallel to fibers, and the interface adhesion is strong enough unless otherwise specified.

Data availability
The raw/processed data required to reproduce these findings cannot be shared at this time as the data also form part of an ongoing study.

Declaration of Competing Interest
The authors declare that they have no known competing financial interests or personal relationships that could have appeared to influence the work reported in this paper.

References

[1] J. Li et al., Science 357 (2017) 378.
[2] J. Li, D.J. Mooney, Nat. Rev. Mater. 1 (2016) 16071.
[3] G.M. Whitesides, Angew. Chem. Int. Edit. 57 (2018) 4258.
[4] D. Rus, M.T. Tolley, Nature 521 (2015) 467.
[5] C. Keplinger et al., Science 341 (2013) 984.
[6] C. Yang, Z. Suo, Nat. Rev. Mater. 3 (2018) 125.
[7] H.-R. Lee et al., Adv. Mater. 30 (2018) 1704403.
[8] D.-H. Kim et al., Science 333 (2011) 838.
[9] T. Someya et al., Nature 540 (2016) 379.
[10] H. Yuk et al., Chem. Soc. Rev. 48 (2019) 1642.
[11] A.S. Khalil, J.J. Collins, Nat. Rev. Genet. 11 (2010) 367.
[12] S.Y. Chin et al., Sci. Robot. 2 (2017) eaah6451.
[13] P. Le Floch et al., ACS Appl. Mater. Interfaces 9 (2017) 25542.
[14] H. Jinno et al., Nat. Energy 2 (2017) 780.
[15] R. Bai et al., Eur. J. Mech. A-Solid 74 (2019) 337.
[16] G.J. Lake et al., Proc. R. Soc. London, Ser. A. Math. Phys. Sci. 300 (1967) 108.
[17] J. Tang et al., Extreme Mech. Lett. 10 (2017) 24.
[18] E. Zhang et al., Soft Matter 14 (2018) 3563.
[19] R. Bai et al., ACS Macro. Lett. 7 (2018) 312.
[20] R. Bai et al., Extreme Mech. Lett. 15 (2017) 91.
[21] W. Zhang et al., Eng. Fract. Mech. 187 (2018) 74.
[22] S. Lin et al., Sci. Adv. 5 (2019) eaau8528.
[23] S. Lin et al., Proc. Natl. Acad. Sci. 116 (2019) 10244.
[24] N. Fleck et al., Acta Metall. Mater. 42 (1994) 365.
[25] J.P. Gong et al., Adv. Mater. 15 (2003) 1155.
[26] E. Ducrot et al., Science 344 (2014) 186.
[27] J.-Y. Sun et al., Nature 489 (2012) 133.
[28] A.M. Bueche, J. Polym. Sci. 25 (1957) 139.
[29] W.-C. Lin et al., Macromolecules 43 (2010) 2554.
[30] W. Zhang et al., ACS Macro. Lett. 8 (2019) 17.
[31] R. Bai et al., Macromol. Rapid Commun. 40 (2019) 1800883.
[32] Z. Wang et al., Proc. Natl. Acad. Sci. 116 (2019) 5967.
[33] P.K. Mallick, Fiber-Reinforced Composites: Materials, Manufacturing, and Design, CRC Press, 2007.
[34] J.D. Walter, Rubber Chem. Technol. 51 (1978) 524.
[35] U.G.K. Wegst et al., Nat. Mater. 14 (2014) 23.
[36] A. Agrawal et al., Acta Biomater. 9 (2013) 5313.
[37] Y. Huang et al., Adv. Funct. Mater. 27 (2017) 1605350.
[38] S. Xia et al., Phys. Rev. Lett. 108 (2012) 196101.
[39] K.-I. Jang et al., Nat. Commun. 6 (2015) 6566.
[40] S.P. Lacour et al., Appl. Phys. Lett. 88 (2006) 204103.
[41] C. Boller, T. Seeger, Materials Data for Cyclic Loading Part D Aluminium and Titanium Alloys, Elsevier, 1987.
[42] G.Y. Wang et al., Intermetallics 12 (2004) 885.
[43] T.A. Schaedler et al., Science 334 (2011) 962.
[44] C. Chen et al., Extreme Mech. Lett. 10 (2017) 50.
[45] Y.B. Kim et al., J. Appl. Polym. Sci. 114 (2009) 3870.
[46] K. Tian et al., Adv. Mater. 29 (2017) 1604827.
[47] N. Bhattacharjee et al., Adv. Mater. 30 (2018) 1800001.
[48] J. Yang et al., Adv. Funct. Mater. (2019) 1901693.
[49] H. Yuk et al., Nat. Commun. 7 (2016) 12028.